Application of X-ray Diffraction Techniques to The Understanding of The Dry Sliding Wear Behaviour of Aluminum and Titanium

by
Zoheir N. Farhat, Ahmet T. Alpas and Derek O. Northwood
Department of Mechanical and Materials Engineering
University of Windsor
Windsor, Ontario, Canada
N9B 3P4

ABSTRACT

Dry sliding wear tests were performed on polycrystalline f.c.c. Al and h.c.p. Ti specimens using a block-on-ring type wear machine with a rotating ring made of 52100 bearing steel. The sliding speed was 0.13 $m.s^{-1}$ and the applied normal load was 10 N. The wear tests were performed on a single specimen in ambient conditions and the texture was evaluated during wear using an X-ray diffraction inverse pole figure technique at a range of sliding distances. Pole density distributions for the [0001] and [111] poles for of Ti and Al, respectively, were then determined from the inverse pole figures. The texture evolution during sliding wear was subsequently related to the friction and wear behaviour. For the aluminum sample, a (111) texture developed parallel to the worn surface with increasing sliding distance (a 6 fold increase in the (111) pole density as the sliding distance increases from 0 to 2714 m). The titanium sample (normal section) which had a preferred orientation with the basal poles, [0001], parallel to the contact surface prior to testing, an increase in wear, i.e. sliding distance, did not change the texture. However, for the transverse section of titanium, the basal pole, [0001], density parallel to the worn surface increased with increasing sliding distance. The shape of the coefficient of friction versus sliding distance curve is strongly influenced by crystallographic texturing. A drop in the coefficient of friction with the progressive development of the [111] and [0001] texture was observed for both Al and Ti (transverse section) specimens, respectively.

Introduction

Although, friction is a time dependent phenomenon, it is commonly reported as an average single value. Friction versus sliding distance (time) curves give the variation of the coefficient of friction as a function of time[1-4]. Until recently[4-9] the time-dependant friction behaviour had not been explored and was still not well understood. Factors such as evolution of crystallographic texture[10] and near-surface work-hardening[5] that takes place during the wear process are reported to influence the friction curve. Only a limited amount of research has been conducted to determine the influence of texturing on friction and wear. Texture evolution during wear often resembles that of a rolling texture[11]. It has been reported[10,12,13] that for hexagonal metals, sliding tends to produce an alignment of basal slip planes (0001) parallel to the worn surface. For fcc metals, Wheeler and Buckley[14] found a (111) texture (the slip plane in fcc) for rubbed copper and nickel. A similar texture evolution during sliding wear for stainless steel and aluminum has been observed by Hirth and Rigney[10]. The influence of texture on the abrasion resistance of Ti-8.5%Al was investigated by Zum-Gahr[15]. Higher wear rates were recorded on surfaces with a basal texture than those with a transverse texture. Similar results were obtained on hexagonal cobalt[15] which suggested that plastic deformation during wear is easier on surfaces showing

basal textures. Static friction between two oriented crystals of copper[16] showed that the coefficient of friction on the (100) face was more than 4 times larger than that on the (111) face. The lower coefficient of friction was attributed to the ease of shearing the crystal parallel to its slip planes.

In the present work, both the crystallographic evolution and tribological properties were examined in order to study the effect of texture development on time-dependent friction and wear transitions.

Experimental Methods

The materials tested were coarse-grained Al and Ti and nanocrystalline Al and Ti films produced by r.f. sputtering method. The grain size of the as-sputtered nanocrystalline Al was varied by annealing at 573 K for the time interval of 10 hrs. in a vacuum sealed quartz tube. Hardness measurements were performed using a nanoindentation system (UMIS 2000). The microstructural and mechanical characterization of all materials tested is summarised in Table 1.

Friction and wear tests were performed under unlubricated sliding conditions using a miniature pin-on-disc type tribometer . The tribometer consists of a specimen holder (disc) rotated by an A.C. motor sliding against a stationary stainless steel (AISI 304) pin. Tests were made under a constant load of 1.0±0.1N and a sliding speed of $1.3X10^{-2}$ $m.s^{-1}$. The instantaneous values of the calibrated normal (N) and tangential (T) forces were measured and the coefficient of friction (μ=T/N) as a function of sliding distance was calculated.The width of the wear track was measured at a regular intervals during the test and the volume loss (V) of the material during wear was calculated according to the ASTM standard G99[17].

Texture measurements during the wear process were made by an X-ray diffraction inverse-pole-figure technique. The purpose of texture measurements was to relate changes in the friction and wear behaviour to the microstructural changes. Dry sliding wear tests were performed on Al and Ti specimens of 5x5 mm^2. For the Ti, the tests were performed on both normal and transverse directions of the disc. A block-on-ring type wear machine was used for these particular experiments. The block-on-ring configuration was chosen over the pin-on-disc wear machine because it provides larger wear surface area for the subsequent X-ray texture analysis. The block-on-disc wear machine consists of a rotating ring, made a of 52100 bearing steel. The sliding speed was set to a $1.3X10^{-1}$ $m.s^{-1}$ and the load was 10 N. The texture development of samples was investigated at selected sliding distances using X-ray diffraction and (0001) and (111) inverse-pole-figures were constructed[18] for Ti and Al, respectively.

To plot an inverse pole figure, the intensities from the sample and those from randomly oriented sample (taken from the Powder Diffraction File for both Al and Ti) were determined. Then a texture coefficient (T.C.) for each (hkil) is calculated using the equation:

$$T.C._i = (I_i / I°_i) / [(1/n) * \sum (I_i / I°_i)] \quad 1$$

where I_i is the intensity of the i^{th} reflection for the textured sample and $I°_i$ is the intensity

of the i^{th} reflection from the randomly oriented sample. The T.C. values are then entered on a stereographic projection. Pole density distribution curves, T.C.(Φ) versus Φ (where the angle Φ is the tilt of a diffraction pole from the [0001] (or [111]) pole), were then determined from the inverse pole figures[19]. A texture index is calculated and plotted as a function of sliding distance for $0 \leq \Phi \leq 30°$,i.e.,

$$\text{Texture index} = \sum_{0}^{35^{\circ}} \text{T.C.}(\Phi)_{\text{average}} \qquad 2$$

Results and Discussion

The coefficient of friction curves (Fig. 1) were characterized by two friction regimes; initially, the coefficient of friction increases rapidly until reaching a peak value μ_p. This was followed by a gradual decrease to a steady-state value $\mu_{s.s}$. The cumulative volume loss versus sliding distance curve also exhibited two distinct regions; initially, the wear rates (slope of the cumulative volume loss versus sliding distance curves) were high (severe wear) but after a certain sliding distance, the slope decreased to a lower value (mild wear). The transition from severe to mild wear generally corresponded to a similar (i.e., about the same sliding distance) transition from the peak to steady state coefficient of friction regime. Friction and wear results are summarised in Table 1.

A preferred crystallographic orientation evolved near the worn surfaces during the wear process. A strong (111) texture progressively develops in the coarse-grained aluminum in the material adjacent to the contact surface (Fig. 2). While the number of the (111) planes making large angles with the contact surface decreases rapidly with increasing sliding distance. Formation of a (111) texture parallel to the worn surface reduces the resistance to the sliding motion since the (111) plane is a slip plane in the fcc aluminum crystal and deformation occurs by shearing of surface layers. In turn, this causes the coefficient of friction to drop to steady state (Fig. 1). A (111) texture parallel to the worn surface is found in aluminum with grain sizes of 16.4 and 43.1 nm even prior to wear (Fig. 3). In fact, the initial texture of nanocrystalline aluminum resembles that of the 1 mm grain size aluminum at a sliding distances > 4000 m. Consequently, the drop in the coefficient of friction ($\Delta\mu_p$ in Table 1) of nanocrystalline aluminum is smaller than that of coarse-grained aluminum.

On the other hand, there is no significant textural changes during wear for coarse-grained titanium. This is expected in light of the fact that prior to wear, the "normal" section of the titanium disc has a strong (0001) texture (Fig. 4). The (0001) planes, being slip planes in the hcp titanium crystal, are parallel to the worn surface and remain at this orientation throughout the wear process. This, in part, explains the constant coefficient of friction ($\Delta\mu_p$=0, see Table 1) exhibited during sliding. On the other hand, sliding wear experiments performed on the "transverse" section of the titanium disc indicate a development of a (0001) texture as sliding progresses. The increase in the texture index ($0 \leq \Phi \leq 30°$) reveals that the texture of the normal section remains essentially constant while the transverse section (initially having no (0001) texture) has undergone a 30% increase (Fig. 5). Hence, a drop in the coefficient of friction ($\Delta\mu_p$=0.4) for the transverse section (Table 1) as a consequence of the (0001) planes become parallel to the contact surface, which in turn, reduces the resistance to sliding. The increase in the texture index for coarse grained aluminum is about 550% (Fig. 5) this is accompanied by a larger drop in the coefficient of friction, $\Delta\mu_p$=1.22, in comparison to coarse-grained titanium.

The initial texture of the as-sputtered titanium (prior to wear) is characterised by a large number of [0001] poles oriented at 90° from the contact surface as opposed to the normal section of coarse-grained titanium. Therefore, as expected, it shows a corresponding drop in the coefficient of friction ($\Delta\mu_p$=0.21) at large sliding distances (Table 1). It should be mentioned here that other factors[20] such as work hardening, topographical and microstructural changes during the wear process would also contribute to the wear and friction transitions.

Conclusions

1. Friction and wear properties of Al and Ti sliding against stainless steel were studied.
2. An inverse-pole-figure technique was employed to monitor the crystallographic texture evolution during wear.
3. The shape of the time-dependent coefficient of friction is strongly influenced by crystallographic texturing of material in the wear track.
4. In general, it is commonly observed that the coefficient of friction rises to a peak value (μ_p) after a short sliding distance then settles down to a steady-state value ($\mu_{s.s}$). Similarly, the wear rate versus sliding distance curves show a transitional behaviour from severe wear to mild wear above a critical sliding distance corresponding to the transition from μ_p to $\mu_{s.s}$.
5. (0001) and (111) textures develop parallel to the worn surface during the sliding wear of titanium and aluminum, respectively. This texture development contributes to the transition from peak to steady state coefficient of friction.

References

1. A. Wang and H. J. Rack, Journal of Materials Science and Engineering, 1991, A147, 211.
2. Y. L. Su and J. S. Lin, Wear, 166(1993)27.
3. T. E. Levine, P. Revesz, W. Mayer and E. P. Giannelis in: Thin Films, Stress and Mechanical Properties IV, Mat. Res. Soc. Sym. Proc., eds., P. H. Townsend, T. P. Weihs and J. E. Sanchez, Pittsburgh, 1993, 308, 635.
4. P. J. Blau, Journal of Tribology, 1987, 109, 537.
5. D. A. Rigney and J. P. Hirth, Wear, 1979, 53, 345.
6. D. Kuhlmann-Wilsdorf, in Fundamentals of Friction and Wear of Materials, ed., D. A. Rigney, ASM, Metals Park Ohio, 1980, 119.
7. N. P. Suh, in Fundamentals of Friction and Wear of Materials, ed., D. A. Rigney, ASM, Metals Park Ohio, 1980, 43.
8. P. J. Blau, Friction and Wear Transitions of Materials, Noyes Publishing,New Jersey, 1989.
9. N. P. Suh, Tribophysics, Prentice-Hall, New Jersey, 1986.
10. J. P. Hirth and D. A. Rigney, in Dislocations in Solids Vol. 6, ed., F. R. Nabarro, North-Holland Publishing, Amsterdam, 1983, 10.
11. R. W. K. Honeycomb, The Plastic Deformation of Metals, 2nd eds., Edward Arnold Ltd., U.K., 1984, 326.
12. V. D. Scott and H. Wilman, Proc. Roy Soc. London, 1958, A247, 353.
13. J. Goddard, H. J. Hacker and H. Wilman, Proc. Phys. Soc., 1962, 80, 77.
14. D. R. Wheeler and D. H. Buckley, Wear, 1975, 33, 65.
15. K. Zum-Gahr, Microstructure and Wear of Materials, Elsevier, Amsterdam, 1987.
16. A. T. Gwathmey and H. Leidheiser and G. P. Smith, Proc. Roy. Soc., 1952, A212, 464.

17. American Society of Testing and Materials, ASTM Standards, G99, ASTM, Philadelphia, (1990)387.
18. G. B. Harris, Comm. National Phys. Lab, 43(1952)113.
19. J. Kearns, AEC Report, Westinghouse Atomic Power Division-Technical Memorandum, WAPD-TM-472, (1965).
20. Z. N. Farhat, Y. Ding, D. O. Northwood and A. T. Alpas, Journal of Materials Science and Engineering, in press.

Table 1. Summary of results on mechanical and tribological properties of materials tested.

Grain size (nm)	μ_p	$\mu_{s.s}$	$\Delta\mu_p$	H (GPa)	W_s($X10^{-3}$) (mm^3/m)	W_m($X10^{-5}$) (mm^3/m)
Aluminum						
16.4	0.62±0.06*	0.25±0.05	0.37±0.11	1.70±0.06	1.82±0.37	2.77±0.39
43.1	0.58±0.03	0.14±0.03	0.44±0.06	1.05±0.12	2.37±0.38	11.3±0.69
10^6	1.34±0.02	0.12±0.06	1.22±0.08	0.30±0.06	10.08±1.78	342.4±6.9
Titanium						
30	0.75±0.04	0.54±0.03	0.21±0.07	10.96±0.20	0.09±0.02	0.32±0.01
$2x10^4$ (normal)	0.69±0.03	0.69±0.04	0.00±0.00	2.57±0.10	2.34±0.66	9.83±0.52
$6x10^4$ (transverse)	1.01±0.04	0.61±0.06	0.40±0.10	2.15±0.12**	----------	----------

μ_p = peak coefficient of friction.
$\mu_{s.s}$ = steady-state coefficient of friction.
$\Delta\mu_p$ = $(\mu_p - \mu_{s.s})$.
H = Hardness using UMIS.
W_s = severe wear rate.
W_m = mild wear rate.
*denotes fluctuation around the mean.
** Vickers hadness.

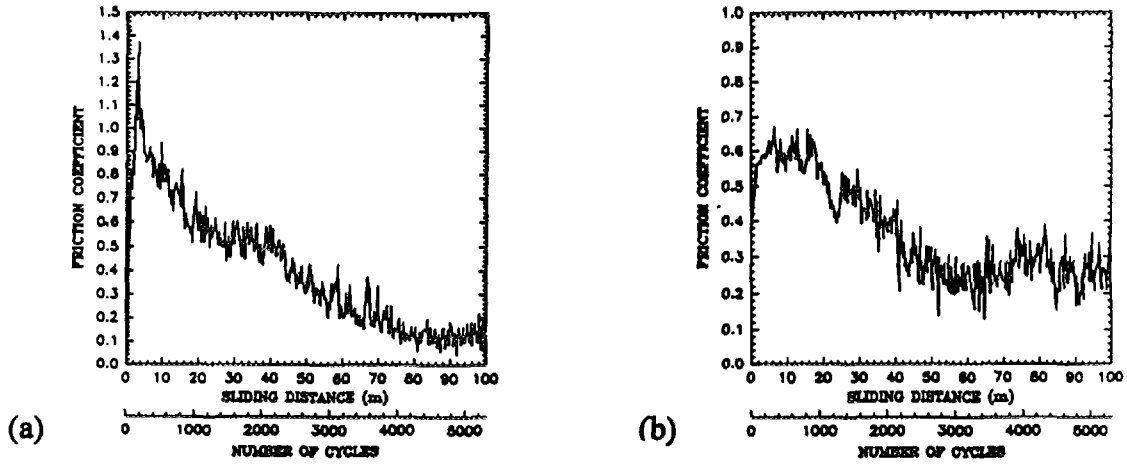

Figure 1. Coefficient of friction versus sliding distance curves obtained using a normal load of 1.0 N and a sliding speed of 1.3×10^{-2} m.s^{-1} under unlubricated sliding conditions for Al of grain size of: (a) 1 mm; (b) 16.4 nm.

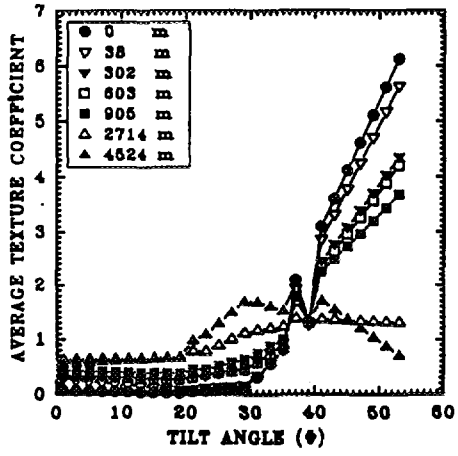

Figure 2. Average texture coefficient versus tilt angle from the reference direction (normal to the worn surface) at different sliding distances for coarse-grained Al.

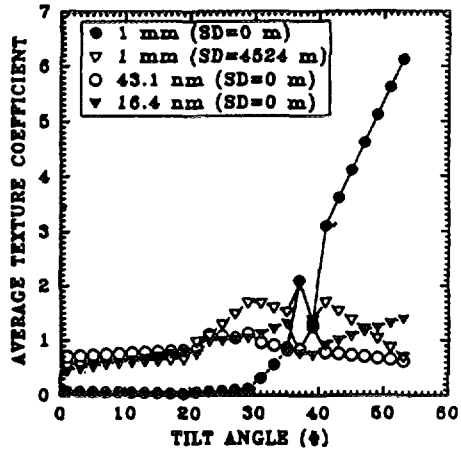

Figure 3. Comparison between the average texture coefficient of coarse-grained and that of nanocrystalline Al.

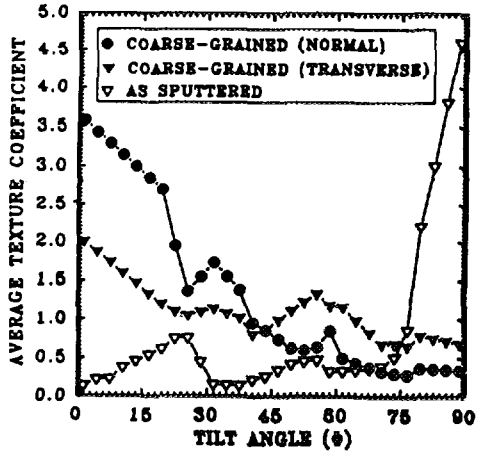

Figure 4. Comparison between the average texture coefficient of coarse-grained (normal and transverse sections) and that of nanocrystalline Ti.

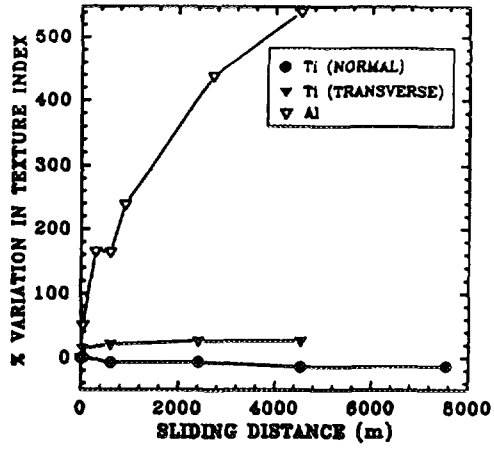

Figure 5. Texture evolution during the wear process as a function of sliding distance.